Blind subspace-based eigenstructure identification under nonstationary excitation using moving sensors

Laurent Mevel, Albert Benveniste, Michèle Basseville, Maurice Goursat

Abstract— **Subspace identification algorithms have proven efficient for performing output-only identification of the eigenstructure of a linear MIMO system subject to uncontrolled, unmeasured, and nonstationary excitation. Such a problem arises in mechanical engineering, for modal analysis of vibrating structures. A common practice there is to collect data from varying sensor locations, using both fixed and moving sensors, in order to mimic the availability of a larger set of sensors. The purpose of this paper is to investigate how subspace-based identification can be adapted to handle such a situation, to prove its consistency under nonstationary excitation, and to report on a real application example.**

Keywords— **Blind eigenstructure identification, nonstationary excitation, subspace algorithms, moving sensors, vibration analysis.**

I. Introduction

Subspace-based linear system identification methods [8], [13], [14] have proven efficient for the identification of the eigenstructure of a linear multi-variable system. An important instance of this problem is structural vibration analysis, based on measurements from accelerometers or strain gauges, where the key issue is to identify vibrating characteristics (modes and modeshapes) of mechanical structures subject to uncontrolled, *unmeasured* and *nonstationary* excitation. A relevant approach to structural analysis has been shown to rely on the modeling of modes and modeshapes through state space representations [11], and the use of *output-only* and *covariance-driven* eigenstructure identification methods [7], [1].

A common practice in vibration analysis is to collect data from varying sensor locations, using both fixed and moving sensors, in order to mimic the availability of a (much) larger set of sensors. Several successive data sets are recorded, with sensors at different locations on the structure. Some of the sensors, called the *reference* sensors, are kept fixed, while the others are moved. This setup, usually referred to as *multi-patch measurements* setup and typically based on about ten sensors, can mimic a situation in which hundreds of sensors are available. Processing multi-patch measurements data for structural analysis is achieved today by performing eigenstructure identification for each record separately, and then merging the results obtained for records corresponding to different sensor pools. However, pole matching may be not easy in practice, and thus the result of eigenvector gluing may not be consistent. Therefore the question arises to perform eigenstructure identification by merging the data of the successive records, and processing them globally, instead of merging the identification results.

This work has been carried out within the framework of Eureka project 1562 Sinopsys (model based **S**tructural monitoring using **IN**-**OP**eration **SYS**tem identification), coordinated by LMS, Leuven, Belgium. L.M., A.B. and M.B. are with Irisa, Campus de Beaulieu, 35042 Rennes Cedex, France. L.M. and A.B. are also with Inria, and M.B. with Cnrs. M.G. is with Inria, BP 105, Rocquencourt, 78153 Le Chesnay Cedex, France. Corresponding author: M.B., basseville@irisa.fr, Tel:+33 2 99 84 7236, Fax:+33 2 99 84 7171.

The purpose of this paper is to investigate how subspace-based identification methods can be adapted to handle a multi-patch measurements setup, in the presence of an unmeasured and nonstationary excitation. In section II, we briefly review output-only covariance-driven subspace identification methods. The mathematical modeling of the multi-patch measurements setup is stated in section III. A first merge of the data is proposed for the stationary excitation case, and shown to fail in the nonstationary one. In section IV, a covariance normalization prior to merge is proposed for the simplified case of record-dependent excitation, and its implementation is given. The fully nonstationary case, in which the excitation is nonstationary within the records, is addressed in section V, where a consistency result is proven. Structural vibration analysis and numerical results for a real application example are reported in section VI. Finally, some conclusions are drawn in section VII.

II. Output-only covariance-driven subspace identification

We consider linear multi-variable systems described by a discrete-time state space model

$$\left\{ \begin{array}{rcl} X_{k+1} &=& F\ X_k \ +\ V_{k+1} \\ Y_k &=& H\ X_k \end{array} \right. \tag{1}$$

where state X and observed output Y have dimensions n and r, respectively, and where the state noise process $(V_k)_k$ is an *unmeasured* Gaussian white noise sequence with zero mean and, in the stationary case, constant covariance matrix Q: $\mathbf{E}(V_k V_{k'}^T) \stackrel{\text{def}}{=} Q\ \delta(k-k')$, where $\mathbf{E}(.)$ denotes the expectation operator. The whiteness assumption on the state noise and the absence of measurement noise in (1) are further discussed in section VI. Let the pairs (λ, Φ_λ) be the eigenvalues and eigenvectors of the state transition matrix F, and define $\varphi_\lambda \stackrel{\text{def}}{=} H\Phi_\lambda$. We assume that the system has no multiple eigenvalues, and thus that the λ's and φ_λ's are pairwise complex conjugate. In particular, 0 is *not* an eigenvalue of state transition matrix F. The collection of pairs $(\lambda, \varphi_\lambda)$ form a canonical parameterization (invariant w.r.t. changes in the state basis) of the pole part of system (1), referred to as the system eigenstructure.

Covariance-driven subspace identification of the $(\lambda, \varphi_\lambda)$'s is based on the following steps[1]. Let $R_i \stackrel{\text{def}}{=} \mathbf{E}(Y_k Y_{k-i}^T)$ and

$$\mathcal{H}_{p+1,q} \stackrel{\text{def}}{=} \begin{pmatrix} R_0 & R_1 & \vdots & R_{q-1} \\ R_1 & R_2 & \vdots & R_q \\ \cdot & \cdot & \vdots & \cdot \\ R_p & R_{p+1} & \vdots & R_{p+q-1} \end{pmatrix} \stackrel{\text{def}}{=} \text{Hank}(R_i) \quad (2)$$

be the theoretical output-covariance and Hankel matrices, respectively. Introduce also the cross-covariance between the state and the observed outputs: $G \stackrel{\text{def}}{=} \mathbf{E}(X_k Y_k^T)$, and the observability and controllability matrices: $\mathcal{O}_p(H,F) \stackrel{\text{def}}{=} \begin{pmatrix} H \\ HF \\ \cdot \\ HF^{p-1} \end{pmatrix}$ and $\mathcal{C}_q(F,G) \stackrel{\text{def}}{=} (G \ FG \ \cdots \ F^{q-1}G)$. Direct computations of the R_i's from model equations (1) lead to

$$R_i = H \ F^i \ G \quad (3)$$

and to the well known factorization [12]

$$\mathcal{H}_{p+1,q} = \mathcal{O}_{p+1}(H,F) \ \mathcal{C}_q(F,G) \quad (4)$$

(In the sequel, we often drop the system matrices orders.)

The observation matrix H is then found in the first block-row of the observability matrix $\mathcal{O}$, whereas exploiting the shift invariance property of $\mathcal{O}$ provides us with the state-transition matrix F, from which the eigenstructure $(\lambda, \varphi_\lambda)$ results. The key feature in factorization (4) which will be elaborated on, is that the left factor $\mathcal{O}$ only depends on the pair (H,F), and thus on the eigenstructure of system (1), whereas the excitation V_k only affects the right factor $\mathcal{C}$ through the cross-covariance matrix G.

The actual implementation of this subspace algorithm has the empirical covariances

$$\widehat{R}_i = 1/N \sum_{k=1}^{N} Y_k \ Y_{k-i}^T \quad (5)$$

substituted for R_i in $\mathcal{H}_{p+1,q}$, yielding the empirical Hankel matrix $\widehat{\mathcal{H}}_{p+1,q}$. How to select the number of lags $(p+q)$ and thus the size of $\widehat{\mathcal{H}}_{p+1,q}$ is discussed in section VI. The SVD of $\widehat{\mathcal{H}}_{p+1,q}$ and its truncation at the desired model order yield, in the *left factor*, an estimate $\widehat{\mathcal{O}}$ for the observability matrix $\mathcal{O}$, from which $(\widehat{H}, \widehat{F})$ and $(\widehat{\lambda}, \widehat{\varphi}_\lambda)$ are recovered as sketched above.

III. Multi-patch subspace identification: stationary excitation

Instead of a single record for the output (Y_k) of system (1), we now have J records

$$\underbrace{\begin{pmatrix} Y_k^{(0,1)} \\ Y_k^{(1)} \end{pmatrix}}_{\text{Record 1}} \ \underbrace{\begin{pmatrix} Y_k^{(0,2)} \\ Y_k^{(2)} \end{pmatrix}}_{\text{Record 2}} \ \cdots \ \underbrace{\begin{pmatrix} Y_k^{(0,J)} \\ Y_k^{(J)} \end{pmatrix}}_{\text{Record } J} \quad (6)$$

[1] Processing output covariance matrices is of interest for very large data sets. The difference between the covariance-driven form of subspace algorithms which we describe and the usual data-driven form is minor, at least for eigenstructure identification [13], [9].

collected successively. Each record j contains data $Y_k^{(0,j)}$ from a fixed *reference* sensor pool, and data $Y_k^{(j)}$ from a *moving* sensor pool. The number of sensors may be different in the fixed and the moving pools, and thus in each record j, the measurement vectors $Y_k^{(0,j)}$ and $Y_k^{(j)}$ may have different dimensions. This is known under the name of multi-patch measurements setup.

To each record j $(1 \leq j \leq J)$ corresponds a state-space realization in the form

$$\begin{cases} X_{k+1}^{(j)} &= F \ X_k^{(j)} + V_{k+1}^{(j)} \\ Y_k^{(0,j)} &= H_0 \ X_k^{(j)} \qquad \text{(reference pool)} \\ Y_k^{(j)} &= H_j \ X_k^{(j)} \qquad \text{(sensor pool n}^o j) \end{cases} \quad (7)$$

with a single state transition matrix F - since the same system is being observed, a fixed observation matrix H_0 for the fixed sensor pool, and a specific observation matrix H_j corresponding to location j of the moving sensor pool.

The problem is to find how to adapt the output-only covariance-driven subspace algorithm of section II in order to identify the eigenstructure of F in (7), on the basis of the measurements (6) which we should merge somehow for this purpose. At this point, two facts should be stressed. First, the cornerstone in section II is factorization (3) which, of course, holds for each of the J records with a *different* left factor H and a *different* right factor G. In particular, even though we do have access to empirical estimates of the covariances $\mathbf{E} \ (Y_k^{(j)} \ Y_{k-i}^{(j)\,T})$ of the moving sensor pool, they are of poor help because their factorizations (3) show up a record-dependent state-output correlation G since the sensors location change. Second, we have no access to cross-record covariances $\mathbf{E} \ (Y_k^{(j')} \ Y_{k-i}^{(j)\,T})$ with $j \neq j'$, since sensor pools j and j' do not record data simultaneously. Thus, we cannot stack all the data sets in a unique vector, otherwise we would have to handle incomplete covariance matrices.

A consequence of those two facts, in the perspective of building a Hankel matrix enjoying a factorization property, is to concentrate on the covariances involving the *reference sensors*. From now on, we thus focus on the two following families of covariances

$$R_i^{0,j} \stackrel{\text{def}}{=} \mathbf{E} \ (Y_k^{(0,j)} \ Y_{k-i}^{(0,j)\,T}), \quad R_i^j \stackrel{\text{def}}{=} \mathbf{E} \ (Y_k^{(j)} \ Y_{k-i}^{(0,j)\,T}) \quad (8)$$

of which we can compute empirical estimates, for lags $i \geq 0$.

A first merge of the data is now proposed for the stationary input excitation case. It is shown to fail in the nonstationary case, even under the simplifying assumption of stationary excitation within the records.

Constant excitation covariance matrix. In the stationary case, the excitation covariance matrix does not depend on record j: $\mathbf{E} \ (V_k^{(j)} V_{k'}^{(j)\,T}) = Q \ \delta(k-k')$, and the cross-covariance between the state and the fixed sensors output $G \stackrel{\text{def}}{=} \mathbf{E}(X_k^{(j)} Y_k^{(0,j)\,T})$ does *not* depend on j either. Therefore, for all the records $j = 1, \ldots, J$ and lags $i \geq 0$, the covariances in (8) factorize, with a constant *right* factor, as

$$\begin{aligned} R_i^{0,j} &= H_0 \ F^i \ G \ \stackrel{\text{def}}{=} \ R_i^0 \\ R_i^j &= H_j \ F^i \ G \end{aligned} \quad (9)$$

Consequently, for each lag $i \geq 0$, we can stack the R_i^j's into a block-column vector

$$R_i^\pi \stackrel{\text{def}}{=} \begin{pmatrix} R_i^0 \\ R_i^1 \\ \vdots \\ R_i^J \end{pmatrix} \tag{10}$$

which factorizes as

$$R_i^\pi = H\ F^i\ G \tag{11}$$

where H is the block-column of observation matrices

$$H \stackrel{\text{def}}{=} \begin{pmatrix} H_0 \\ H_1 \\ \vdots \\ H_J \end{pmatrix} \tag{12}$$

Therefore, the Hankel matrix filled with those column-stacked covariances[2] factorizes as

$$\mathcal{H}^\pi \stackrel{\text{def}}{=} \text{Hank}(R_i^\pi) \ = \ \mathcal{O}(H, F)\ \mathcal{C}(F, G) \tag{13}$$

and the algorithm described in section II for the standard case can be applied to $\mathcal{H}^\pi$. In other words, when the input excitation is stationary, we can proceed as if we had the full set of sensor data available altogether, instead of sensor pools with varying locations. In this case, direct application of the subspace algorithm to the column-stacked covariances (10) is a simple solution to the multi-patch output-only eigenstructure identification problem.

Record-dependent excitation covariance matrix. If we assume that the input excitation covariance matrix depends on the record index j: $\mathbf{E}\ (V_k^{(j)}\ V_{k'}^{(j)\,T}) = Q_j\ \delta(k-k')$, the cross-covariance matrix $G_j \stackrel{\text{def}}{=} \mathbf{E}(X_k^{(j)} Y_k^{(0,j)\,T})$ also *depends on* j. Hence, for $j = 1, \ldots, J$ and $i \geq 0$, factorizations (9) now write with a record-dependent G

$$\begin{aligned} R_i^{0,j} &= H_0\ F^i\ G_j & (14)\\ R_i^j &= H_j\ F^i\ G_j & (15) \end{aligned}$$

and vector R_i^π of stacked covariances defined in (10) no longer factorizes as in (11). As a consequence, brute force application of subspace algorithm by stacking the R_i^j's is not an appropriate solution to the eigenstructure identification problem in the case of record-dependent input excitation noise. To circumvent this difficulty, the idea is to *normalize* the covariance matrices (14)-(15) to make them looking as if they were obtained with the same excitation.

IV. Nonstationary excitation: data normalization

For finding the appropriate normalization, we perform different covariance stacking operations for the data from the reference and moving sensors, respectively. In what follows, we use the generic notations introduced in section II.

[2]This Hankel matrix has $(J+1)$ times as many rows as columns.

Reference sensors. Thanks to (14), all the Hankel matrices built on the data delivered by the reference sensors of the J records factorize with the same *left* factor as

$$\mathcal{H}_{0,j} \stackrel{\text{def}}{=} \text{Hank}(R_i^{(0,j)}) \ = \ \mathcal{O}(H_0, F)\ \mathcal{C}(F, G_j) \tag{16}$$

We can thus proceed as follows. Let $R_i^0 \stackrel{\text{def}}{=} \left(R_i^{0,1}\ R_i^{0,2}\ \ldots\ R_i^{0,J}\right)$ be the block-row vector of the entire set of reference data covariances. It factorizes as

$$R_i^0 = H_0\ F^i\ G, \quad \text{where } G \stackrel{\text{def}}{=} (\ G_1\ G_2\ \ldots\ G_J) \tag{17}$$

Thus the Hankel matrix filled with those row-stacked covariances[3] also factorizes as

$$\mathcal{H}_0 \stackrel{\text{def}}{=} \text{Hank}(R_i^0) \ = \ \mathcal{O}(H_0, F)\ \mathcal{C}(F, G) \tag{18}$$

Note that matrix $\mathcal{H}_0$ can be obtained by interleaving the block-columns of the J Hankel matrices $\mathcal{H}_{0,j}$ in (16). Assume that pair (H_0, F) is observable. Then, partitioning the right factor $\mathcal{C}$ of (18) in the same manner as G in (17), we recover the right factors $\mathcal{C}(F, G_j)$ of (16) for all $j = 1, \ldots, J$. Note that processing the reference data $Y_k^{(0,j)}$ *altogether*, on the basis of the *single* Hankel matrix factorization (18), is mandatory for making sure that we deal with the *same* state bases in (7).

Moving sensors. Thanks to (15), the Hankel matrix built on the covariances of the data $Y_k^{(j)}$ from the moving sensor pool in record j enjoys a record-dependent factorization

$$\mathcal{H}_j \stackrel{\text{def}}{=} \text{Hank}(R_i^j) \ = \ \mathcal{O}(H_j, F)\ \mathcal{C}(F, G_j) \tag{19}$$

Assume that, for all j, the pair (F, G_j) is controllable[4] and that, up to a permutation on the record indexes, $\mathcal{C}(F, G_1)$ is the best conditioned controllability matrix among the $\mathcal{C}(F, G_j)$'s. For all j, we define the normalized matrices

$$\overline{\mathcal{H}}_j \stackrel{\text{def}}{=} \mathcal{H}_j \left(\mathcal{C}^T(F, G_j) \left(\mathcal{C}(F, G_j)\mathcal{C}^T(F, G_j)\right)^{-1} \mathcal{C}(F, G_1)\right) \tag{20}$$

We note that $\overline{\mathcal{H}}_j$ coincides with the Hankel matrix $\text{Hank}(\overline{R}_i^j)$ built on covariances $\overline{R}_i^j$ which factorize as

$$\overline{R}_i^j = H_j\ F^i\ G_1 \tag{21}$$

Therefore, we can now proceed as in the case of constant excitation covariance matrix. For each lag $i \geq 0$, we define the block-column stacked covariances

$$\overline{R}_i \stackrel{\text{def}}{=} \begin{pmatrix} \overline{R}_i^0 \\ \overline{R}_i^1 \\ \vdots \\ \overline{R}_i^J \end{pmatrix}, \quad \text{where } \overline{R}_i^0 \stackrel{\text{def}}{=} R_i^{0,1} = H_0\ F^i\ G_1 \tag{22}$$

Thanks to (21), those stacked covariances $\overline{R}_i$ behave as R_i^π defined in (10): they factorize as $\overline{R}_i = HF^iG_1$, with H

[3]This Hankel matrix has J times as many columns as rows.

[4]This is a reasonable assumption, it just tells that, while the excitation may change, we need it to excite all the modes of the system, for each data set.

defined in (12). Therefore, the Hankel matrix filled with those column-stacked covariances[5] factorizes as

$$\overline{\mathcal{H}} \stackrel{\text{def}}{=} \text{Hank}(\overline{R}_i) = \mathcal{O}(H, F)\ \mathcal{C}(F, G_1) \tag{23}$$

Note that matrix $\overline{\mathcal{H}}$ can be obtained by interleaving the block-rows of $\overline{\mathcal{H}}_0 \stackrel{\text{def}}{=} \text{Hank}(\overline{R}_i^0) = \mathcal{H}_{0,1}$ and of the J matrices $\overline{\mathcal{H}}_j$ defined in (20). Thanks to (23), the algorithm given in section II can be applied to $\overline{\mathcal{H}}$.

Algorithm. For implementing the above reasoning, we propose the following algorithm, where J is the number of records and $\widehat{M}$ denotes an empirical estimate of matrix M.

- Build the J Hankel matrices $\widehat{\mathcal{H}}_{0,j} = \text{Hank}(\widehat{R}_i^{(0,j)})$ from the reference sensor data.
- Build $\widehat{\mathcal{H}}_0$ by interleaving the block-columns of the J matrices $\widehat{\mathcal{H}}_{0,j}$'s $(j = 1, \ldots, J)$.
- SVD-decompose $\widehat{\mathcal{H}}_0$. Keep only the right factor $\mathcal{C}(F, G)$ in (18), and call it just $\mathcal{C}$.
- Partition $\mathcal{C}$ into $\mathcal{C} \stackrel{\text{def}}{=} (\mathcal{C}_1\ \mathcal{C}_2\ \ldots\ \mathcal{C}_J)$ as G in (17). Assume $\mathcal{C}_1$ is the best conditioned.
- Compute the normalizing factors $\left(\mathcal{C}_j^T\ (\mathcal{C}_j \mathcal{C}_j^T)^{-1}\ \mathcal{C}_1\right)$.
- Build the J Hankel matrices $\widehat{\mathcal{H}}_j = \text{Hank}(\widehat{R}_i^j)$ from the moving sensor data.
- Compute the J normalized matrices $\widehat{\overline{\mathcal{H}}}_j \stackrel{\text{def}}{=} \widehat{\mathcal{H}}_j\ \left(\mathcal{C}_j^T\ (\mathcal{C}_j \mathcal{C}_j^T)^{-1}\ \mathcal{C}_1\right)$. Define $\widehat{\overline{\mathcal{H}}}_0 \stackrel{\text{def}}{=} \widehat{\mathcal{H}}_{0,1}$.
- Build $\widehat{\overline{\mathcal{H}}}$ by interleaving the block-rows of the $(J+1)$ matrices $\widehat{\overline{\mathcal{H}}}_j$'s $(j = 0, \ldots, J)$.
- Apply the algorithm of section II to $\widehat{\overline{\mathcal{H}}}$.

The following comments are in order. First, the computational complexity of this algorithm does *not* depend on the number J of records, since the smallest dimension of the two Hankel matrices $\widehat{\mathcal{H}}_0$ and $\widehat{\overline{\mathcal{H}}}$ to be decomposed depends only on the number of reference sensors. Second, the interleaving of the block-rows of the $\widehat{\overline{\mathcal{H}}}_j$'s can be done even when the number of sensors in the moving pools is *not* constant: the measurement vectors $Y_k^{(j)}$ and $Y_k^{(j')}$ may have different dimensions. Third, we do not need to compute explicitly the G_j matrices, since only the right factors $\mathcal{C}(F, G_j)$ in (19) are needed for computing $\widehat{\overline{\mathcal{H}}}_j$ in (20).

V. Nonstationary excitation within the records

In section IV, we have assumed stationary excitation within each record, with record-dependent covariance matrix. This is a reasonable approximation when the environmental conditions are slowly time-varying. But a more realistic assumption is that the excitation covariance matrix: $\mathbf{E}\ (V_k^{(j)} V_{k'}^{(j)\,T}) = Q_{k,j}\ \delta(k - k')$ is *time-varying within each record*. Hence the output data of the multi-patch measurements setup (7) cannot be assumed stationary within each individual record, and we cannot apply the argument of section IV. Nevertheless, the algorithm described in that section can still be applied with little modification, and can be proven consistent, as shown next using the results of [4].

[5] This Hankel matrix has $(J+1)$ times as many rows as columns.

The rationale of the formal results below is the following. When the excitation is nonstationary, the empirical covariance matrices $\widehat{R}_i$ in (5) no longer converge to some well defined underlying R_i when the sample size N goes to infinity, and may vary in some arbitrary way. Nevertheless, the approximate factorization still holds, for N large:

$$\widehat{R}_i = H\ F^i\ \widehat{G} + o(N) \tag{24}$$

where: $\widehat{G} = 1/N\ \sum_{k=1}^{N} X_k\ Y_k^T$ and $o(N)$ goes to zero when the sample size N goes to infinity. One of the assumptions for this to hold formalizes the requirement that all the modes of the structure should be excited. Property (24) is the key step in proving the consistency.

The formal results are the following. For $j = 1, \ldots, J$, let $\mathcal{I}_j$ be the finite set of sample points in record j, let $K_j \stackrel{\text{def}}{=} |\mathcal{I}_j|$ be the number of samples, and define the following second order empirical moments

$$\begin{aligned}
A_j(K_j) &\stackrel{\text{def}}{=} 1/(2\ K_j) \sum_{k \in \mathcal{I}_j} \left(\|Y_k^{(0,j)}\|^2 + \|Y_k^j\|^2 \right) \\
G_j(K_j) &\stackrel{\text{def}}{=} 1/A_j(K_j) \sum_{k \in \mathcal{I}_j} X_k^{(j)}\ Y_k^{(0,j)\,T} \\
R_i^{0,j}(K_j) &\stackrel{\text{def}}{=} 1/A_j(K_j) \sum_{k \in \mathcal{I}_j} Y_k^{(0,j)}\ Y_{k-i}^{(0,j)\,T} \\
R_i^j(K_j) &\stackrel{\text{def}}{=} 1/A_j(K_j) \sum_{k \in \mathcal{I}_j} Y_k^j\ Y_{k-i}^{(0,j)\,T}
\end{aligned} \tag{25}$$

Consider the following assumptions, identical to conditions C1 and C2 of section II.A of [4].

C1: $\lim_{K_j \to +\infty} A_j(K_j) = +\infty$ with probability 1.
C2: The excitation covariance matrix $Q_{k,j}$ is uniformly bounded from above, in k (and thus in (finite) j).
Note that condition **C1** is a very mild request stating that, for each individual record j, the system is sufficiently excited. The following result is proved in the first step of the proof of theorem 1 in [4][Sec.III.A]:

Theorem 1: Under conditions **C1-C2**, we have

$$\begin{aligned}
R_i^{0,j}(K_j) &= H_0\ F^i\ G_j(K_j) + o(K_j) \\
R_i^j(K_j) &= H_j\ F^i\ G_j(K_j) + o(K_j)
\end{aligned}$$

where matrix $o(K)$ goes to zero when K goes to infinity. Theorem 1 expresses that (14)-(15) hold asymptotically. Consider now the following additional assumptions.

C3: For every j and K_j large, the n-th (in decreasing order) singular value of the controllability matrix $\mathcal{C}_j(K_j) \stackrel{\text{def}}{=} \mathcal{C}_q(F, G_j(K_j))$ is asymptotically uniformly bounded from below with probability 1.
C4: For every j, the pair (H_j, F) is observable: rank $\mathcal{O}_p(H_j, F) = n$.
Condition **C3**, which coincides with condition **C3** of [4][Sec.II.A], means that the pair $(F, G_j(K_j))$ is asymptotically uniformly controllable for every j and K_j large.

Introduce the Hankel matrix $\mathcal{H}^j \stackrel{\text{def}}{=} \text{Hank}(R_i^j(K_j))$ and the normalized matrix

$$\overline{\mathcal{H}}^j \stackrel{\text{def}}{=} \mathcal{H}^j \left(\mathcal{C}_j^T \; (\mathcal{C}_j \; \mathcal{C}_j^T)^{-1} \; \mathcal{C}_1\right) \tag{26}$$

where $\mathcal{C} \stackrel{\text{def}}{=} (\mathcal{C}_1 \; \mathcal{C}_2 \; \dots \; \mathcal{C}_J)$ is the right factor of $\mathcal{H}^0$, and $\mathcal{H}^0$ is built by interleaving the block-columns of the J matrices $\mathcal{H}^{0,j} \stackrel{\text{def}}{=} \text{Hank}(R_i^{0,j}(K_j))$. Note that, as in (20), $\overline{\mathcal{H}}^j$ is an Hankel matrix built on covariances which we note $\overline{R}_i^j$. The following theorem holds.

Theorem 2: Under conditions **C1-C4**, those covariances enjoy the approximate factorization:

$$\overline{R_i^j} \;=\; H_j \; F^i \; G_1(K_1) + o(K_1) \tag{27}$$

where matrix $o(K_1)$ goes to zero when K_1 goes to infinity.

Proof. For all the K_j large, define $R_i^j \stackrel{\text{def}}{=} H_j F^i G_j(K_j)$, $\mathcal{H}_j \stackrel{\text{def}}{=} \text{Hank}(R_i^j)$ and $\overline{\mathcal{H}}_j \stackrel{\text{def}}{=} \text{Hank}(H_j \; F^i \; G_1(K_1))$. With these notations, theorem 1 writes $R_i^j(K_j) = R_i^j + o(K_j)$ and we have the following relation for the Hankel matrices

$$\overline{\mathcal{H}}_j = \mathcal{H}_j \left(\mathcal{C}_j^T(K_j) \; (\mathcal{C}_j(K_j) \; \mathcal{C}_j^T(K_j))^{-1} \; \mathcal{C}_1(K_1)\right) \tag{28}$$

For proving (27), it is sufficient to prove that, for all j and for K_j large, the following holds:

$$\overline{\mathcal{H}}^j = \overline{\mathcal{H}}_j + o(\min_j K_j) \tag{29}$$

To prove (29), we note that (26) and (28) result in

$$\begin{aligned} \overline{\mathcal{H}}^j - \overline{\mathcal{H}}_j \;&=\; \mathcal{H}^j \underbrace{\left(\mathcal{C}_j^T \; (\mathcal{C}_j \; \mathcal{C}_j^T)^{-1} \; \mathcal{C}_1\right)}_{\mathcal{F}^j} \\ &- \;\; \mathcal{H}_j \underbrace{\left(\mathcal{C}_j^T(K_j) \; (\mathcal{C}_j(K_j) \; \mathcal{C}_j^T(K_j))^{-1} \; \mathcal{C}_1(K_1)\right)}_{\mathcal{F}_j} \end{aligned} \tag{30}$$

Thanks to condition **C3**, controllability matrices $\mathcal{C}_1$ and $\mathcal{C}_j$ are uniformly bounded from below, for K_1 and K_j large, and matrix $(\mathcal{C}_j \; \mathcal{C}_j^T)^{-1}$ is uniformly bounded from above. This and theorem 1 together imply that, for K_j large,

$$\mathcal{H}^j = \mathcal{H}_j + o(K_j) \;, \quad \mathcal{F}^j = \mathcal{F}_j + o(\min_j K_j) \tag{31}$$

Equations (30) and (31) together prove (29). This concludes the proof of the theorem.

Theorems 1 and 2 ensure that the method of section IV applies, provided that we use the $R_i^{0,j}(K_j)$'s and $R_i^j(K_j)$'s in (25) as empirical estimates of the covariances. Furthermore, the following consistency can be proven, as in [4].

Theorem 3: Under conditions **C1-C4**, the algorithm of section IV is consistent: there exists a sequence of matrices T, with T and T^{-1} uniformly bounded, such that $T^{-1} \; \widehat{F} \; T \to F, \quad \widehat{H} \to H$ with probability 1.

Since we have assumed that the system has no multiple eigenvalues and because the eigenstructure is a continuous function of the pair (H, F), this theorem also ensures [4] the consistency of the eigenstructure estimate $(\widehat{\lambda}, \widehat{\varphi}_\lambda)$.

VI. Structural vibration analysis example

As mentioned in the introduction, structural vibration analysis of complex mechanical structures and rotating machines subject to ambient excitation is an important instance of eigenstructure identification. These systems are subject to fast and *unmeasured* variations in their environment, and thus the input excitation is typically turbulent in nature and *nonstationary.* Typical examples are offshore structures subject to swell, buildings subject to wind or earthquake, bridges, dams, wings subject to flutter in flight, and turbines subject to steam turbulence, friction in bearings, and imperfect balancing [11], [3]. In this section, we describe the application of the multi-patch subspace identification method of section IV to structural vibration analysis. We introduce the modeling issues, and then we report some numerical results obtained on a real example.

A. Modeling

We assume that the behavior of the mechanical system can be described by a stationary linear dynamical system, and that, in the frequency range of interest, the input forces can be modeled as a nonstationary white noise. This results in the following matrix differential equation :

$$\left\{ \begin{array}{rcl} M\ddot{\mathcal{Z}}(t) + C\dot{\mathcal{Z}}(t) + K\mathcal{Z}(t) &=& \nu(t) \\ Y(t) &=& L\mathcal{Z}(t) \end{array} \right. \tag{32}$$

where t denotes continuous time, M, C, K are the mass, damping and stiffness matrices respectively, (high dimensional) vector $\mathcal{Z}$ collects the displacements or accelerations of the degrees of freedom of the structure; the external (non measured) force ν is modeled as a nonstationary white noise with time-varying covariance matrix $Q_\nu(t)$, measurements are collected in the (low dimensional) vector Y, and matrix L indicates which components of the state vector are actually measured (where the sensors are located). Sinusoidal or colored excitation noise can be encompassed as well [11]. How the presence and nature of excitation and measurement noises are handled in practice, when using an algorithm non encompassing them, is addressed in subsection VI-B.

The parameters (M, C, K) cannot be recovered from measured outputs. Hence, identifiable parameters are introduced. These are the modes or eigen-frequencies μ, and the modeshapes or eigenvectors ψ_μ, solutions of:

$$(M\mu^2 + C\mu + K) \; \Psi_\mu = 0 \;, \quad \psi_\mu = L \; \Psi_\mu \tag{33}$$

Sampling model (32) at rate $1/\tau$ yields the discrete time state space model (1), where the state and the output are :

$$X_k = \begin{pmatrix} \mathcal{Z}(k\tau) \\ \dot{\mathcal{Z}}(k\tau) \end{pmatrix}, \quad Y_k = Y(k\tau), \tag{34}$$

the state transition and observation matrices are :

$$F = e^{\mathcal{L}\tau}, \; \mathcal{L} = \begin{pmatrix} 0 & I \\ -M^{-1}K & -M^{-1}C \end{pmatrix}, \; H = (\; L \; 0 \;),$$

and where state noise V_{k+1} is zero-mean, white, with covariance matrix: $Q_{k+1} = \int_{k\tau}^{(k+1)\tau} e^{\mathcal{L}s} \; \widetilde{Q}(s) \; e^{\mathcal{L}^T s} ds$, where

$\widetilde{Q}(s) = \begin{pmatrix} 0 & 0 \\ 0 & M^{-1}Q_\nu(s)M^{-T} \end{pmatrix}$. The modal parameters in (33) are equivalently found in the eigenstructure (λ, Φ_λ) of F: $e^{\tau\mu} = \lambda$, $\psi_\mu = \varphi_\lambda \stackrel{\text{def}}{=} H\ \Phi_\lambda$. Because of the structure of the state in (34), the eigenvectors are pairwise complex conjugate. The frequency and damping coefficient are recovered from a given eigenvalue λ through: Frequency $= a/(2\pi\ \tau)$, Damping $= 100\ |b|/\sqrt{a^2+b^2}$, $a = |\arctan \Im(\lambda)/\Re(\lambda)|$, $b = \ln|\lambda|$.

Vibration analysis is thus stated as the problem of identifying the eigenstructure of the state transition matrix of a linear dynamic system with nonstationary state noise [6], [5]. State X and output Y have dimensions $n = 2\dim \mathcal{Z}$ and r respectively, with r often (much) smaller than n.

B. Numerical results

We now report some numerical results obtained with the multi-patch subspace algorithm proposed in section IV. Before proceeding, some comments are in order on the practical use of the classical (monoreference and full covariance) subspace identification algorithm of section II.

Some practical issues in subspace eigenstructure identification. The selection of the model order, and thus of the size of the Hankel matrices on one hand, and the handling of the presence and nature of excitation and measurement noises on the other hand, are two major practical issues which we address now.

As stressed in [11], [3], [9], when few sensors are available, a number of modes which is much smaller than the number of solutions of (33), but much larger than the number of sensors, can be identified. In order to extract the modes from the data, we have to apply the subspace method with an increasing SVD truncation order and to look for the relevant modes in the frequency band of interest. Since the subspace method yields a set of modes with both structural – from the structure *and* the excitation – and spurious mathematical modes, we have to derive a practical way to distinguish between the two types of modes. Fortunately, spurious modes tend to vary from one model order to the next. That is why usage suggests to plot the frequencies against SVD truncation order, in a so-called stabilization diagram [9]. Moreover, the stability of the modes is evaluated on the frequencies, the damping coefficients, *and* the mode-shape components. Numerous experiments with the classical subspace method have shown that :

- It is of no practical help to select for $\mathcal{H}_{p+1,q}$ in (2) other values than $q = p+1$. The number of lags $2p$ for the data covariances should be large (typically more than two hundreds in the experiments below),
- The number of modes should be overestimated, because modes tend to stabilize, and even to show up, for high orders. In other words, the SVD in the algorithm of section II should be truncated at an order much greater than the 'theoretical' order, that is $2m/r - 1$, where m is the number of desired modes and r is the number of sensors.

An excitation noise at a single constant frequency is recognized as a pole by the algorithm of section II, designed under the assumption of a white excitation noise. Such a pole can be eliminated provided that an *a priori* information is available. This is the case of the harmonics of the rotation speed for rotating machines with load unbalancing. Similarly, a colored excitation noise can easily be eliminated provided that its poles are (significantly) more damped than those of the structure. It is also a common finding that the poles of the structure tend to stabilize when the Hankel matrix order is increased, whereas those of the excitation mostly do not. A nonstationary excitation is actually a favorable situation, since the averaging performed in (25) for computing G tends to whiten the noise. This is the case of a chirp-like nonstationary excitation.

If a measurement noise is enforced in (34), or (1), it can be encompassed by shifting the lags of the covariances used for filling the Hankel matrices [13], [2].

Real application example. The proposed method has been applied to the Swiss Z24 bridge, a benchmark of the BRITE/EURAM project SIMCES on identification and monitoring of civil engineering structures, for which EMPA[6] has carried out tests and data recording. The response of the bridge to traffic excitation under the bridge has been measured in 135 points, mainly in the vertical and transverse directions, and sampled at 100Hz. Because at most 19 sensors were available, 9 data sets have been recorded, each containing the measurements from 4 fixed and 15 moving sensors. However, it is not recommended to merge data recorded under too different temperature and traffic conditions [10], and to mix different directions [11]. Therefore, for investigating the experimental properties of the proposed multi-patch subspace algorithm, we have selected $J = 2$ records from sensors in the vertical direction, with one reference sensor, and two moving sensors in the first record, and only one moving sensor in the second record. Each signal contains 65535 samples. As mentioned above, processing more records would have affected the required memory size, but *not* the computational complexity. Also, it is of interest to investigate the practical relevance of the conceptual capability of the proposed algorithm to handle records with different numbers of moving sensors.

The classical subspace algorithm of section II, based on full data covariances and on $q = 128$, has been applied separately to each record, which contain 3 and 2 sensors, respectively. The results are displayed in Fig. 2 and 3, where frequencies (ordinate) are displayed for increasing SVD truncation order (abscissa), in a stabilization diagram which symbols are explained in Fig. 1. Some typical values of estimated modes which can be extracted from these diagrams are displayed in Table I.

TABLE I
Classical subspace identification - Some estimated modes .

Mode	1	2	3	4
Frequency (Hz)	4	5.3	10.3	12

[6]Swiss Federal Laboratories for Materials Testing and Research.

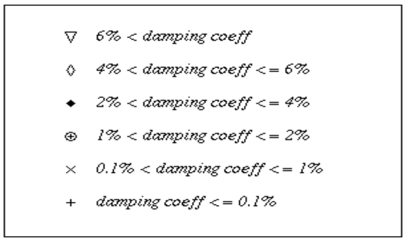

Fig. 1. Meaning of the symbols in Fig. 2 to 4.

Multi-patch subspace eigenstructure identification. The multi-patch subspace identification algorithm of section IV, based on partial covariances[7] (8) and on $q = 128$, has been applied to the data from the two records. Since the Hankel matrix $\overline{\mathcal{H}}$ is built on stacked covariances (22), its SVD truncation order should be taken no greater than $128 \times 1/(1+2+1) = 32$. The results are displayed in Fig. 4, which shows up several improvements over Fig. 2 and 3, on several aspects. For large enough truncation order:

- Spurious modes disappear: around 1 Hz, for example;
- True modes appear and stabilize faster and fluctuate less in the diagrams: around 5.3 Hz for example. This mode is very difficult to extract, because of low excitation for this frequency. In both classical identifications, it appears very late in the diagrams and has low stability, whereas those two issues are overcome in the multi-patch trial.
- Some modes, not identified on Fig. 2 and 3, now show up in a stable diagram: 9.8 Hz for example.
- The damping of the true modes is more accurately estimated, at lower orders than before, allowing to separate true and wrong modes among the stabilized ones: a wrong mode appears at 7 Hz with a high damping, whereas the true mode at 4 Hz appears with a low damping;
- The multi-patch method extracts seven modes in the range $0 - 11$ Hz. Two of these modes, at 1.8 Hz and 7 Hz, are recognized as spurious, because of high damping, and of the information available on the benchmark. The five other modes are those given in Table I plus the mode at 9.8 Hz, and come from the structure. They appear in many (classical and multi-patch) diagrams during the whole year.

Fig. 4 is a remarkably clear diagram which, above a truncation order of 15, is cleaned from all spurious poles, even those which tend to stabilize in Fig. 2 and 3.

What the proposed multi-patch subspace identification algorithm is not capable of is to separate modes of the structure from the modes corresponding to the non–white excitation, but the classical subspace identification procedure is unable to achieve that either. Nevertheless, the new algorithm appears to perform well at extracting modes which appear only in some diagrams, for example modes which are not very well excited all the time. This feature is important in practice, and should hopefully be confirmed in further numerical investigations.

[7]Note that these covariance matrices are column vectors, since only one reference sensor is available in each of the two records.

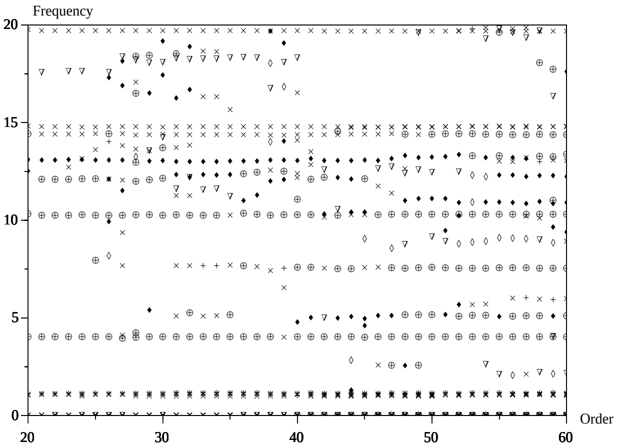

Fig. 2. Classical subspace identification: first record (3 sensors).

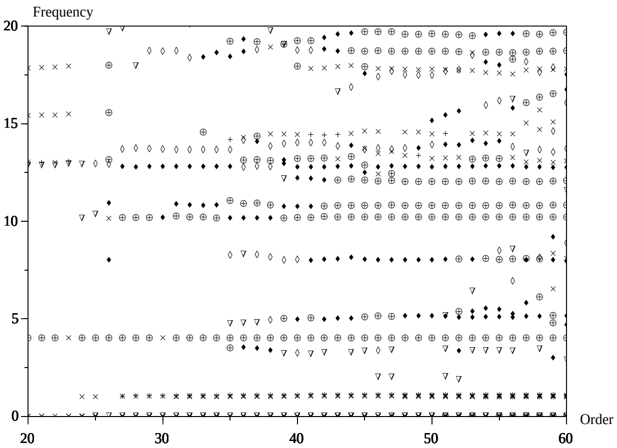

Fig. 3. Classical subspace identification: second record (2 sensors).

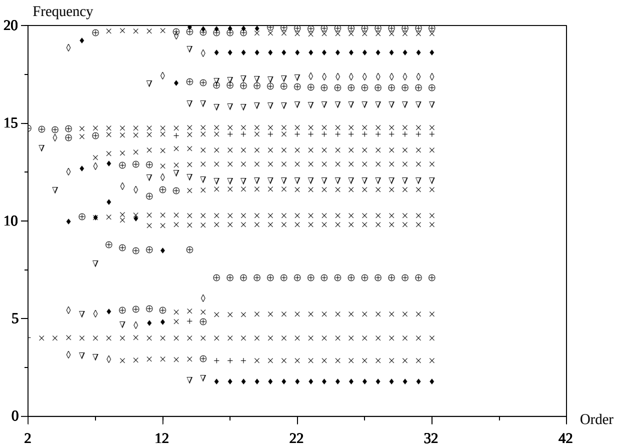

Fig. 4. Multi-patch subspace identification with the two records.

VII. Conclusion

We have discussed the multi-patch measurements setup for blind eigenstructure identification. This type of setup is popular for instance in vibration mechanics, where several moving sensors mimic the availability of a much larger set of sensors. The proposed identification method consists in merging the data first and processing them globally using an output-only covariance-based subspace algorithm. This has to be contrasted with classical multi-patch identification, which is usually performed by merging identification results obtained on the different records. The presence of an unmeasured and nonstationary excitation makes the issue of output data merging nontrivial. The key idea of the proposed method is a suitable normalization of the output covariances. This method has been proved to provide us with consistent estimates of the eigenstructure, even under nonstationary excitation. Some numerical results on one real example have been reported, which highlight the potential benefits of the proposed method. First, the method efficiently merges data by smoothing out the diagrams, rejecting spurious and instable frequencies. Second, applying the multi-patch method over time is expected to smooth out further the effect of nonstationary excitation. The actual stability of the multi-patch diagrams makes the proposed multi-patch method a good candidate for a future automated identification procedure. Finally, the main benefit of the proposed method is the extraction of the modeshapes, for which no result could be provided in section VI, because of lack of information about the sensor location on the structure. This is the topic of further experimental investigations.

References

[1] M. Abdelghani, M. Goursat, T. Biolchini, L. Hermans and H. Van der Auweraer, "Performance of output-only identification algorithms for modal analysis of aircraft structures", *IMAC-XVII, Int. Modal Analysis Conf.*, Kissimmee, FL, Feb.1999.

[2] M. Basseville, M. Abdelghani and A. Benveniste, "Subspace-based fault detection algorithms for vibration monitoring", *Automatica,* vol.36, no 1, pp.101-109, 2000.

[3] M. Basseville, A. Benveniste, B. Gach-Devauchelle, M. Goursat, D. Bonnecase, P. Dorey, M. Prevosto and M. Olagnon, "Damage monitoring in vibration mechanics: issues in diagnostics and predictive maintenance", *Mech. Syst. Sign. Proc.*, vol.7, n.5, pp.401-423, 1993.

[4] A. Benveniste and J-J. Fuchs, "Single sample modal identification of a nonstationary stochastic process", *IEEE Trans. Automat. Contr.*, vol.30, n.1, pp.66-74, 1985.

[5] F. Deblauwe, R.J. Allemang and D.L. Brown, "The polyreference time domain technique", *IMAC-V, Int. Modal Analysis Conf.*, pp. 832-845, 1987.

[6] D.J. Ewins, *Modal Testing: Theory and Practice*, Research Studies Press, Letchworth, Hertfordshire, UK, 1984.

[7] L. Hermans and H. van der Auweraer, "Modal testing and analysis of structures under operational conditions: industrial applications", *Mech. Syst. Sign. Proc.*, vol.13, n.2, pp.193-216, 1999.

[8] B. Ottersten, M. Viberg and T. Kailath, "Analysis of subspace fitting and ML techniques for parameter estimation", *IEEE Trans. Sign. Proc.*, vol.40, pp.590-599, 1992.

[9] B. Peeters and G. de Roeck, "Reference-based stochastic subspace identification for output-only modal analysis", *Mech. Syst. Sign. Proc.*, vol.13, n.6, pp.855-878, 1999.

[10] B. Peeters and G. de Roeck, "One year monitoring of the Z24-bridge: environmental effects versus damage events", *IMAC-XVIII, Int. Modal Analysis Conf.*, San Antonio, TX, Feb.2000.

[11] M. Prevosto, M. Olagnon, A. Benveniste, M. Basseville, G. Le Vey, "State-space formulation, a solution to modal parameter estimation", *Jal Sound and Vibr.*, vol.148, n.2, pp.329-342, 1991.

[12] P. Stoïca and R.L. Moses, *Introduction to Spectral Analysis*, Prentice Hall, 1997.

[13] P. Van Overschee and B. De Moor, *Subspace Identification for Linear Systems: Theory, Implementation, Applications*, Kluwer, 1996.

[14] M. Viberg and B. Ottersten, "Sensor array processing based on subspace fitting", *IEEE Trans. Sign. Proc.*, vol.39, no 5, pp.1110-1121, 1991.

Laurent Mevel is with IRISA, Rennes, F., where he is currently Chargé de Recherches at INRIA (French National Institute for Research in Computer Science and Automatic Control). He graduated from University of Rennes in 1997, where he received a Ph.D. in Applied Mathematics in the field of statistical inference for hidden Markov models. Since then, he has been working on identification and detection of partially hidden stochastic systems, with application to vibration mechanics.

Albert Benveniste is with IRISA, Rennes, F., where he is Directeur de Recherche at INRIA. He has been working on automatic control and signal processing in the area of adaptive and change detection algorithms for time-varying systems, with applications to data communications and fault detection. He now concentrates on in-operation structural identification and diagnostics for vibration mechanics, and on fault detection for large, distributed systems with application to telecommunications networks. He has also been involved in the definition of and investigations on the Signal synchronous language for the design of safety critical embedded systems, and in foundations for object-oriented software development for large telecommunications switching systems. He has co-authored with M. Métivier and P. Priouret the book *Adaptive Algorithms and Stochastic Approximations.*

Michèle Basseville is with IRISA, Rennes, F., where she is Directeur de Recherche at CNRS (Centre National de la Recherche Scientifique). Her main domain of interest is the detection of changes in parametric models of signals and dynamical systems, and its application to both recognition-oriented signal processing, and fault detection and isolation for monitoring industrial processes. She has been co-editor, together with Albert Benveniste, of the collective monograph *Detection of Abrupt Changes in Signals and Dynamical Systems*, LNCIS no 77. She is co-author, together with Igor V. Nikiforov, of the book *Detection of Abrupt Changes - Theory and Application.*

Maurice Goursat is with INRIA, Rocquencourt, F. The main interests of his group (METALAU scientific project) are in automatic control, stochastic control and development of related software (free software SCILAB). His present research areas are in monitoring and diagnosis for vibrating structures and control of traffic.